

Synthesis, Properties, and Reactivity of Bis-BN Phenanthrenes: Stepwise Bromination of the Main Scaffold

Lingjian Zi, Jinyun Zhang, Chenglong Li, Yi Qu, Bin Zhen, Xuguang Liu,* and Lei Zhang*


 Cite This: <https://dx.doi.org/10.1021/acs.orglett.0c00021>


Read Online

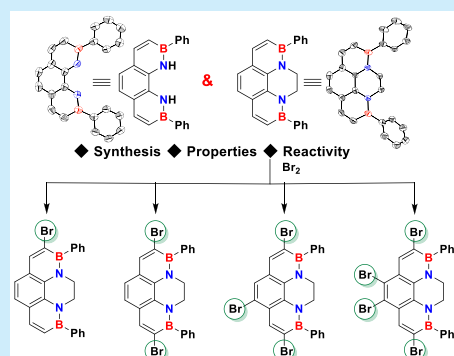
ACCESS |

Metrics & More

Article Recommendations

Supporting Information

ABSTRACT: Two bis-BN phenanthrenes have been synthesized. Their photophysical properties are different from those of the reported mono-BN phenanthrenes. Moreover, the stepwise bromination of bis-BN phenanthrene **8** gave a series of brominated bis-BN phenanthrenes, with all of the mono-, di-, tri-, and tetrabrominated bis-BN phenanthrenes being successfully isolated and characterized. In addition, preliminary results showed that mono- and dibrominated species can be further functionalized by cross-coupling reactions.



Embedding a boron atom into polycyclic aromatic hydrocarbons (PAHs) is an effective way to alter their structural and electronic properties.¹ In particular, BN/CC isosterism resulted in boron/nitrogen-containing PAHs (BN-PAHs), in which the boron and nitrogen atoms have complementary electron-accepting and -donating properties, and they have attracted great attention due to their potential to create new optoelectronic materials.² The mono-BN PAHs are the most common examples of BN-PAHs,³ whereas bis-BN PAHs have often existed in larger sized PAHs.⁴ In terms of bis-BN PAHs in small-size PAHs (three aromatic rings or fewer), only one single example of bis-BN anthracene has been reported.^{4a} In BN-PAHs with more than one BN unit, the fundamental question is the effect of the number of BN units on their chemical and photophysical properties.

Phenanthrene, which is the isomer of linear anthracene, is of great interest to organic and material chemists.⁵ In total, six mono-BN phenanthrene derivatives have been reported to date (Figure 1). The first BN-phenanthrene was reported by the Dewar group in 1958.^{6a} The BN-phenanthrene isomer **2** was also reported by Dewar group,^{6b} and Vaquero and coworkers improved the synthesis of **2** using ring-closing metathesis as the key step.^{7a-c} BN-phenanthrene **3** with an internal BN unit was synthesized by the Piers group using platinum-catalyzed annulation relations.⁸ Wang's group reported the BN-phenanthrene **4** by a photoelimination reaction.⁹ Very recently, Vaquero^{7d,e} and our group¹⁰ independently reported the BN-phenanthrenes **5** and **6** with a BN unit on the terminal ring of phenanthrene. Despite the recent progress in the study of the synthesis and properties of mono-BN phenanthrenes, BN-phenanthrenes beyond the mono-BN isosteres have remained elusive (Figure 1). In this Letter, we describe the synthesis and

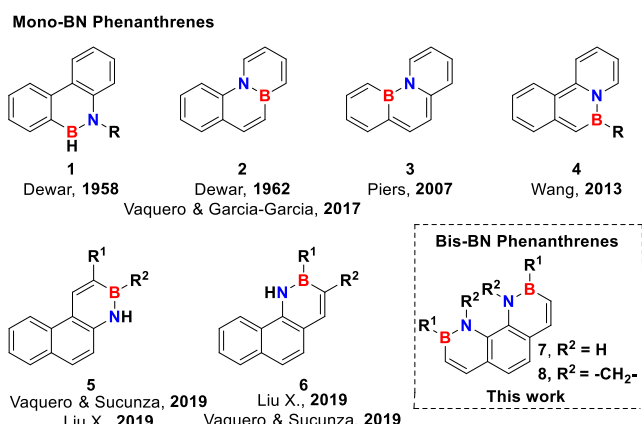


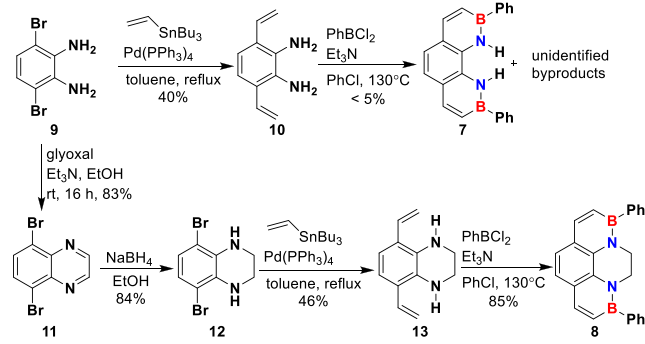
Figure 1. Reported BN-phenanthrenes and this work.

properties of two bis-BN phenanthrenes **7** and **8** (Figure 1, bottom right corner). We found that the properties and reactivities of bis-BN phenanthrenes are intriguingly different from those of mono-BN phenanthrenes.

The synthesis of bis-BN phenanthrenes **7** and **8** is shown in Scheme 1. 3,6-Dibromobenzene-1,2-diamine¹¹ was used as the starting material. Two-fold Stille cross coupling of **9** with tributyl(vinyl)tin yielded the 3,6-divinylbenzene-1,2-diamine

Received: January 8, 2020

Scheme 1. Synthetic Route to bis-BN Phenanthrenes 7 and 8



10 in moderate yield. Intramolecular cyclization of **9** with two equivalents of dichlorophenylborane (PhBCl_2) produced bis-BN phenanthrene **7** in low yield (<5%), along with unidentified byproducts. An attempt to isolate and purify the byproducts failed. To avoid the formation of a byproduct, we decided to connect the two nitrogen atoms with an ethylene bridge (Scheme 1, bottom). Condensation of **10** with glyoxal followed by hydrogenation of the resulting 5,8-dibromoquinoxaline **11** furnished 5,8-dibromo-1,2,3,4-tetrahydroquinoxaline **12**. Stille cross coupling of **12** with tributyl(vinyl)tin gave 5,8-divinyl-1,2,3,4-tetrahydroquinoxaline **13**. Borylative cyclization of **13** with PhBCl_2 produced bis-BN phenanthrene **8** with an ethylene bridge sitting in between two nitrogen atoms, which can also be viewed as bis-BN dihydropyrene, in good yield (85%). We found that both **7** and **8** are stable in air and could be purified by chromatography on silica gel. Attempts toward the dehydrogenation of **8** to get the fully aromatic bis-BN pyrene failed (Scheme S17).

To understand the effects of the location and number of BN units on the aromaticity of bis-BN phenanthrenes, we performed nucleus-independent chemical shifts (NICS) calculations (Figure 2);¹² parental mono-BN phenanthrene **6**

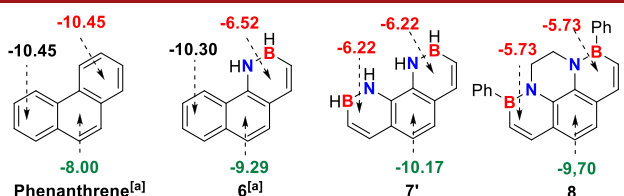


Figure 2. NICS(1) values of phenanthrene, mono-BN phenanthrene **6**, and bis-BN phenanthrenes **7'** and **8** determined at the B3LYP/6-311+G(2d,p) level of theory. ^[a]The NICS(1) values of phenanthrene and **6** are adopted from ref 10.

and carbonaceous phenanthrene were included for direct comparison.¹⁰ The NICS(1) values of the BN rings in **7'** ($\text{B}-\text{H}$, -6.22) and **8** (-5.73) are less negative than those in **6** (-6.52), indicating that the BN rings in bis-BN phenanthrenes have smaller aromaticity. The NICS(1) values of the middle ring of **7'** (-10.17) and **8** (-9.70) are more negative than those of the corresponding ring in carbonaceous phenanthrene (-8.00) and **6** (-9.29), which indicates that the middle rings of bis-BN phenanthrenes **7'** and **8** have stronger aromaticity.

The structures of bis-BN phenanthrenes **7** and **8** were further confirmed by X-ray single-crystal analysis (Figure 3). The typical bond lengths and dihedral angles are shown in Table 1. B–N bond lengths in **7** (1.421(4), 1.418(4) Å) and **8**

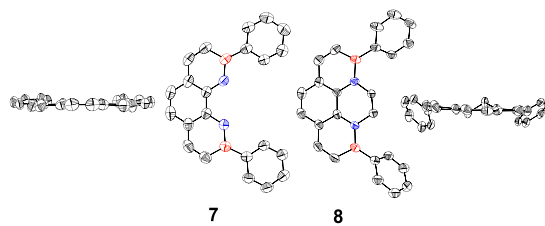


Figure 3. Solid-state structures of bis-BN-phenanthrenes **7** and **8** with views parallel and perpendicular to the polycyclic planes. Thermal ellipsoids are set at the 50% probability level. H atoms have been omitted for clarity.

Table 1. Representing Bond Lengths and Dihedral Angles of bis-BN Phenanthrenes **7 and **8****

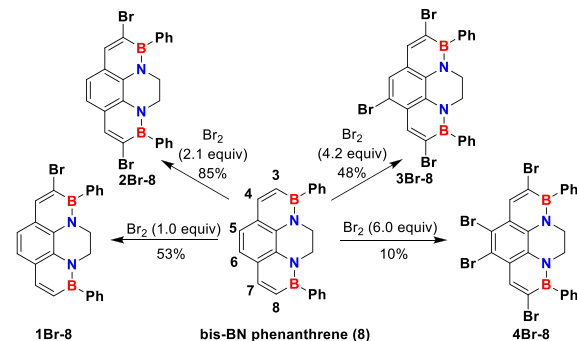
	B1–N1 B2–N2	B–C endo	B–C exo	N–C endo	dihedral angle ^a
7	1.421(4)	1.526(3)	1.555(4)	1.379(3)	4.5°
	1.418(4)	1.518(4)	1.576(4)	1.385(3)	6.8°
8	1.437(8)	1.540(9)	1.583(9)	1.422(7)	48.2°
	1.449(8)	1.545(9)	1.582(9)	1.401(7)	44.0°

^aDihedral angle between the B-phenyl and the main framework of bis-BN phenanthrene plane.

(1.437(8), 1.449(8) Å) are much shorter than the typical B–N single bond (1.56 Å), indicating a distinct double-bond character (1.403(2) Å).¹³ Specifically, the B–N bond lengths of **7** (1.421(4), 1.418(4) Å) are shorter than the B–N bond lengths in **8** (1.437(8), 1.449(8) Å), which is in line with the more negative calculated NICS(1) values of **7'** (-6.22) compared with those of **8** (-5.73). The inner-ring B–C bonds of **7** (1.526(3), 1.518(4) Å) and **8** (1.540(9), 1.545(9) Å) are shorter than the typical B–C single-bond covalent radius (1.58 Å), which indicates its double-bond character as well.¹³ Interestingly, the dihedral angles between the phenyl group attached to boron and the main scaffold of **7** (4.5 and 6.8°) are quite small. In contrast, the phenyl groups on boron are twisted and deviated from the main backbones by 48.2 and 44.0° in **8**, presumably due to the bulky steric effect of the relatively larger CH_2 group attached to the nitrogen atom in **8** (Figure 3 and Table 1).

We then turn our interest to investigating the bromination of bis-BN phenanthrene **8** (Scheme 2). As expected, we found that the bromination products of **8** are dependent on the ratio between **8** and Br_2 used. The bromination of **8** took place exclusively at the α -carbon adjacent to boron when using fewer than two equivalents of Br_2 . Specifically, the mono-brominated

Scheme 2. Stepwise Bromination of bis-BN Phenanthrene **8**



product (**1Br-8**) could be isolated as the major product when using 1.0 equiv of Br_2 (53%). Further increasing Br_2 to 2.1 equiv, the dibrominated product (**2Br-8**) became the major product (85%). When using more than two equivalents of Br_2 , the site-selective tribromination (**3Br-8**) and tetra-bromination (**4Br-8**) of the **8** were observed. After the reaction conditions were optimized, we found that using 4.2 equiv of Br_2 gave the tribrominated product (**3Br-8**) as the major product (48%), along with a trace amount of the mono- and dibrominated products, which can be carefully isolated by chromatography. The tetrabrominated product (**4Br-8**) (10%) could be isolated when using 6.0 equiv of Br_2 along with some unidentified byproducts. We did not isolate any further brominated products in the reaction system.

The solid-state structures of mono- (**1Br-8**), di- (**2Br-8**), and tetra-brominated (**4Br-8**) bis-BN phenanthrene derivatives were successfully confirmed by X-ray single-crystal analysis (Tables S12–S20), which confirmed the regioselectivity of the bromination reactions. An attempt to grow single crystals of tribrominated bis-BN phenanthrene **3Br-8** failed. Notably, the reactivity of bis-BN phenanthrene **8** toward bromination is different from the reactivity of mono-BN phenanthrenes **2**^{7a} and **5**,^{7d,10} in which bromination exclusively occurs at the α -carbon adjacent to boron. With regards to mono-BN phenanthrene **6**, mono-^{7e,10} and dibrominated¹⁰ products could be isolated, and no further bromination was observed. The different behaviors of bis-BN phenanthrene **8** toward bromination highlight the influence of the number and the location of the BN unit on the reactivity of BN phenanthrenes.

Resonance structures can be used to rationalize the activation of C-3, C-5, C-6, and C-8 positions of **8** (Figure 4). Computational studies of brominated intermediates are

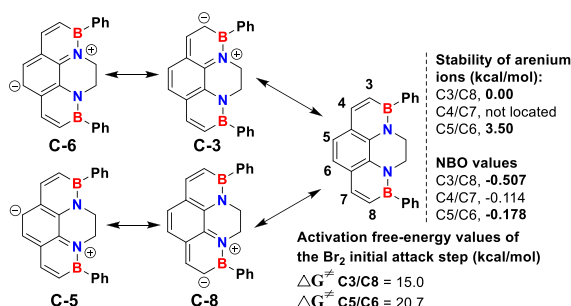


Figure 4. Resonance structures of bis-BN phenanthrene **8** (left) and the calculated stability of arenium ions, corresponding to the attack of Br^+ on different positions of **8**, NBO values, and activation energies determined at the B3LYP/6-311+G(2d,p) level of theory (right).

equally informative in rationalizing the site selectivity observed. We performed theoretical calculations on the relative energies of the arenium ions formed after the addition of bromine to **8** (Figure 4 and Figures S7–S11). The arenium ion intermediate generated by Br^+ attacking at the carbon (C-3/C-8) adjacent to boron was treated as the zero energy reference, which is also the most electron-rich position at which the bromination of 1,2-azaborine^{14a} or BN-naphthalene^{14b} took place. The second lowest-lying arenium ion was observed at C-5/C-6 (3.50 kcal/mol), in line with the site-selective tri- or tetra-bromination results observed experimentally. The C-4/C-7 positions are not located theoretically. The activation free-energy values of the Br_2 initial attack of each position were also calculated ($\text{C}3/\text{C}8 = 15.0$ kcal/mol; $\text{C}5/\text{C}6 = 20.7$ kcal/mol). Natural bond

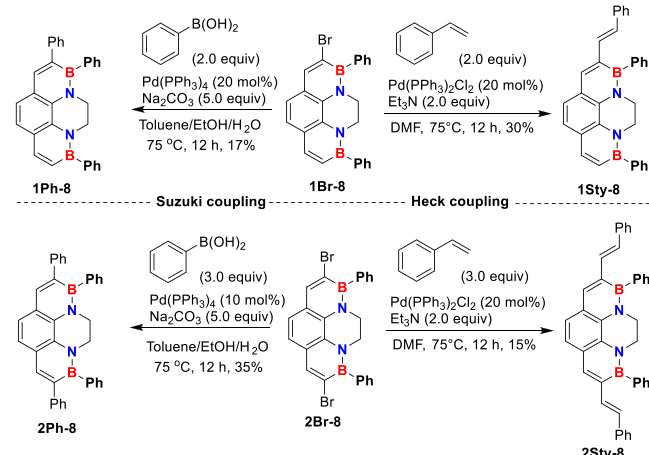
orbital (NBO) charge analyses¹⁵ on **8** demonstrated that the electron density value increases in the order of C4/C7 ($-0.114 < \text{C}5/\text{C}6 < \text{C}3/\text{C}8$ (-0.507)), which should correlate more directly with the observed regioselectivity. The calculated activation energy values and transition states of each step for the formation of mono- (15.0 kcal/mol), di- (17.0 kcal/mol), tri- (24.5 kcal/mol), and tetra-brominated (25.5 kcal/mol) bis-BN phenanthrene derivatives and details of the calculation can be found in the Supporting Information (Figures S8–S11), which is consistent with experimental observation that bromination occurs in a stepwise manner.

We also studied the photophysical properties of bis-BN phenanthrenes **7** and **8**, and we found that the ethylene bridge in **8** has a negligible influence on its absorption and emission energy (Figure S1). Both **7** and **8** showed blue-shifted absorption spectra and red-shifted emission spectra compared with mono-BN phenanthrene **6** (B-Ph) (Figure S1 and Table S1).¹⁰ Furthermore, solvent polarity had little effect on the absorption and emission energies of **7** and **8** (Figure S3). The absolute quantum yields of **8** ($\Phi_{\text{pl}} = 0.19$) are more than three times those of **7** ($\Phi_{\text{pl}} = 0.06$), and both of the values are smaller than that of **6** (B-Ph, $\Phi_{\text{pl}} = 0.85$). The differences in their photophysical properties of **7/8** and mono-BN phenanthrene **6** again highlight the tremendous effect of the number of BN units on the properties of the BN-phenanthrenes. The UV-vis absorption and emission spectra of **1Br-8**, **2Br-8**, **3Br-8**, and **4Br-8** are also recorded (Figure S2 and Table S1).

Aryl halides are widely used in the transition-catalyzed cross-coupling reactions.¹⁶ The cross-coupling reaction of halogenated BN-PAHs is an effective way to further tune their photophysical properties.^{2a,7,10,14b,17} To our delight, Suzuki and Heck cross coupling of **1Br-8/2Br-8** with phenylboronic acid or styrene produced the corresponding coupling products in low yield (Scheme 3).¹⁹ Attempts to utilize the tribrominated (**3Br-8**) and tetra-brominated (**4Br-8**) bis-BN phenanthrenes as cross-coupling partners resulted in complex reaction mixtures.

The direct comparison of the photophysical properties of **1Ph-8**, **2Ph-8**, **1Sty-8**, and **2Sty-8** is shown in Figure 5 and Table 2. (See also Table S1.). The absorption bands of **1Ph-8**, **2Ph-8**, **1Sty-8**, and **2Sty-8** are bathochromically shifted in the

Scheme 3. Further Functionalization of **1Br-8** and **2Br-8**^a



^aReaction conditions were not optimized.

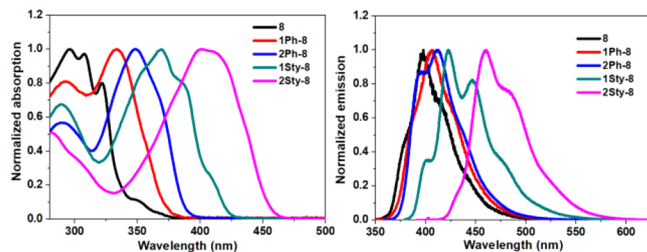


Figure 5. Normalized absorption (left) and emission spectra (right) of **8**, **1Ph-8**, **2Ph-8**, **1Sty-8**, and **2Sty-8** in dichloromethane at a concentration of 10^{-5} M.

Table 2. Photophysical Properties of 8, 1Ph-8, 2Ph-8, 1Sty-8, and 2Sty-8

comp	λ_{abs} (nm) ^a	ϵ ($M^{-1} \text{ cm}^{-1}$)	$\lambda_{\text{em}} (\lambda_{\text{ex}})$ (nm) ^a	Φ_{pl} ^b	EG^{optc}
8	307	25076	397 (322)	0.19	3.25
1Ph-8	333	24674	406 (333)	0.21	3.19
2Ph-8	348	45922	411 (348)	0.60	3.10
1Sty-8	369	30746	423 (369)	0.74	2.89
2Sty-8	400	62469	460 (400)	0.88	2.66

^aRefer to the highest-intensity peak maxima values. ^bAbsolute quantum yield in dichloromethane. ^cOptical band gap $EG^{\text{opt}} = 1240/\lambda_{\text{onset}}$.

order of **1Ph-8** < **2Ph-8** < **1Sty-8** < **2Sty-8** (Figure 5, left), demonstrating the extension of the π -conjugation by the introduction of benzene or styrene moieties. The trend of the emission fluorescence maxima of **1Ph-8**, **2Ph-8**, **1Sty-8**, and **2Sty-8** is consistent with the trend of the UV-vis absorption spectra (Figure 5, right).

In addition, four derivatives **1Ph-8** (0.21), **2Ph-8** (0.60), **1Sty-8** (0.74), and **2Sty-8** (0.88) displayed higher quantum yields than the “parental” bis-BN phenanthrene **8** (0.19). The band gaps estimated from the absorption onsets were found to be 3.19, 3.10, 2.89, and 2.66 eV for **1Ph-8**, **2Ph-8**, **1Sty-8**, and **2Sty-8**, respectively (Table 2). These numbers are qualitatively in agreement with the calculated values (Tables S4 and S5).

In summary, we have successfully synthesized two bis-BN phenanthrenes. The aromaticities of the bis-BN phenanthrenes were quantified by experimental and computational studies. Notably, the number of the BN unit has a significant effect on the reactivity of the BN phenanthrene toward bromination, which was further explained by density functional theory calculations. The stepwise bromination of bis-BN phenanthrene **8** gave a series of brominated compounds. Preliminary results showed that the mono- and dibrominated bis-BN phenanthrenes can be further functionalized by cross-coupling reactions, which can further tailor the photophysical properties of these bis-BN phenanthrenes. Further studies using these bis-BN phenanthrenes as building blocks in organic material are currently underway in our laboratory.

■ ASSOCIATED CONTENT

Supporting Information

The Supporting Information is available free of charge at <https://pubs.acs.org/doi/10.1021/acs.orglett.0c00021>.

Full details of the synthesis of bis-BN phenanthrenes **7** and **8**, NMR spectra, UV-vis and photoluminescence data, X-ray crystallographic data, and theoretical calculations (PDF)

Accession Codes

CCDC 1974591–1974596 and 1975062 contain the supplementary crystallographic data for this paper. These data can be obtained free of charge via www.ccdc.cam.ac.uk/data_request/cif, or by emailing data_request@ccdc.cam.ac.uk, or by contacting The Cambridge Crystallographic Data Centre, 12 Union Road, Cambridge CB2 1EZ, UK; fax: +44 1223 336033.

■ AUTHOR INFORMATION

Corresponding Authors

Xuguang Liu – Tianjin Key Laboratory of Organic Solar Cells and Photochemical Conversion, Tianjin Key Laboratory of Drug Targeting and Bioimaging, School of Chemistry and Chemical Engineering, Tianjin University of Technology, Tianjin 300384, People’s Republic of China; Key Laboratory of Synthetic and Self-Assembly Chemistry for Organic Functional Molecules, Shanghai Institute of Organic Chemistry, Chinese Academy of Sciences, Shanghai 200032, People’s Republic of China; orcid.org/0000-0002-7859-3139; Email: xuguangliu@tjut.edu.cn

Lei Zhang – School of Science, Tianjin Chengjian University, Tianjin 300384, People’s Republic of China; orcid.org/0000-0003-0100-8357; Email: zanglei-chem@tcu.edu.cn

Authors

Lingjian Zi – Tianjin Key Laboratory of Organic Solar Cells and Photochemical Conversion, Tianjin Key Laboratory of Drug Targeting and Bioimaging, School of Chemistry and Chemical Engineering, Tianjin University of Technology, Tianjin 300384, People’s Republic of China

Jinyun Zhang – Tianjin Key Laboratory of Organic Solar Cells and Photochemical Conversion, Tianjin Key Laboratory of Drug Targeting and Bioimaging, School of Chemistry and Chemical Engineering, Tianjin University of Technology, Tianjin 300384, People’s Republic of China

Chenglong Li – Tianjin Key Laboratory of Organic Solar Cells and Photochemical Conversion, Tianjin Key Laboratory of Drug Targeting and Bioimaging, School of Chemistry and Chemical Engineering, Tianjin University of Technology, Tianjin 300384, People’s Republic of China

Yi Qu – Tianjin Key Laboratory of Organic Solar Cells and Photochemical Conversion, Tianjin Key Laboratory of Drug Targeting and Bioimaging, School of Chemistry and Chemical Engineering, Tianjin University of Technology, Tianjin 300384, People’s Republic of China

Bin Zhen – Tianjin Key Laboratory of Organic Solar Cells and Photochemical Conversion, Tianjin Key Laboratory of Drug Targeting and Bioimaging, School of Chemistry and Chemical Engineering, Tianjin University of Technology, Tianjin 300384, People’s Republic of China

Complete contact information is available at:

<https://pubs.acs.org/10.1021/acs.orglett.0c00021>

Notes

The authors declare no competing financial interest.

■ ACKNOWLEDGMENTS

We gratefully acknowledge the financial support from the Natural Science Foundation of Tianjin (17JCZDJC37700, 18JCQNJC06900), the National Natural Science Foundation of China (21502140), Tianjin University of Technology, and the Shanghai Institute of Organic Chemistry (K2015-10). We

also thank the Training Project of Innovation Team of Colleges and Universities in Tianjin (TD13-5020).

■ REFERENCES

- (1) (a) Stępień, M.; Gońska, E.; Żyła, M.; Sprutta, N. *Chem. Rev.* **2017**, *117*, 3479–3716. (b) Narita, A.; Wang, X.; Feng, X.; Müllen, K. *Chem. Soc. Rev.* **2015**, *44*, 6616–6643. (c) Hirai, M.; Tanaka, N.; Sakai, M.; Yamaguchi, S. *Chem. Rev.* **2019**, *119*, 8291–8331. (d) Parke, S. M.; Boone, M. P.; Rivard, E. *Chem. Commun.* **2016**, *52*, 9485–9505.
- (2) (a) Liu, Z.; Marder, T. B. *Angew. Chem.* **2008**, *120*, 248–250; *Angew. Chem., Int. Ed.* **2008**, *47*, 242–244. (b) Bosdet, M. J. D.; Piers, W. E. *Can. J. Chem.* **2009**, *87*, 8–29. (c) Campbell, P. G.; Marwitz, A. J. V.; Liu, S.-Y. *Angew. Chem.* **2012**, *124*, 6178–6197; *Angew. Chem., Int. Ed.* **2012**, *51*, 6074–6092. (d) Abbey, E. R.; Liu, S.-Y. *Org. Biomol. Chem.* **2013**, *11*, 2060–2069. (e) Ashe, A. J., III *Organometallics* **2009**, *28*, 4236–4248. (f) Wang, X.; Wang, J.; Pei, J. *Chem. - Eur. J.* **2015**, *21*, 3528–3539. (g) Morgan, M. M.; Piers, W. E. *Dalton. Trans.* **2016**, *45*, 5920–5924. (h) Helten, H. *Chem. - Eur. J.* **2016**, *22*, 12972–12982. (i) Wang, J. Y.; Pei, J. *Chin. Chem. Lett.* **2016**, *27*, 1139–1146. (j) Bélanger-Chabot, G.; Braunschweig, H.; Roy, D. K. *Eur. J. Inorg. Chem.* **2017**, *2017*, 4353–4368. (k) Giustra, Z. X.; Liu, S.-Y. *J. Am. Chem. Soc.* **2018**, *140*, 1184–1194. (l) Wang, J. *Univ. Chem.* **2017**, *32*, 1–6. (m) Huang, J.; Li, Y. *Front. Chem.* **2018**, *6*, 1–22. (n) Huang, J.; Li, Y. *Front. Chem.* **2018**, *6*, 341–362. (o) McConnell, C.; Liu, S.-Y. *Chem. Soc. Rev.* **2019**, *48*, 3436–3453.
- (3) (a) Sun, C. J.; Wang, N.; Peng, T.; Yin, X.; Wang, S.; Chen, P. *Inorg. Chem.* **2019**, *58*, 3591. (b) Ando, M.; Sakai, M.; Ando, N.; Hirai, M.; Yamaguchi, S. *Org. Biomol. Chem.* **2019**, *17*, 5500–5504. (c) Liu, Z.; Ishibashi, J. S. A.; Darrigan, C.; Dargelos, A.; Chrostowska, A.; Li, B.; Vasiliu, M.; Dixon, D. A.; Liu, S.-Y. *J. Am. Chem. Soc.* **2017**, *139*, 6082–6085. (d) Liu, X.; Wu, P.; Li, J.; Cui, C. *J. Org. Chem.* **2015**, *80*, 3737–3744.
- (4) (a) Ishibashi, J. S. A.; Marshall, J. L.; Mazière, A.; Lovinger, G. J.; Li, B.; Zakharov, L. N.; Dargelos, A.; Gracia, A.; Chrostowska, A.; Liu, S.-Y. *J. Am. Chem. Soc.* **2014**, *136*, 15414–15421. (b) Morgan, M. M.; Patrick, E. A.; Rautiainen, J. M.; Tuononen, H. M.; Piers, W. E.; Spasyuk, D. M. *Organometallics* **2017**, *36*, 2541–2551. (c) Zhuang, F. D.; Sun, Z. H.; Yao, Z. F.; Chen, Q. R.; Huang, Z.; Yang, J. H.; Wang, J. Y.; Pei, J. *Angew. Chem., Int. Ed.* **2019**, *58*, 10708–10712. (d) Wang, X.; Lin, H.; Lei, T.; Yang, D.; Zhuang, F.; Wang, J.; Yuan, S.; Pei, J. *Angew. Chem., Int. Ed.* **2013**, *52*, 3117–3120. (e) Wang, X.; Zhuang, F.; Wang, R.; Wang, X.; Cao, X.; Wang, J.; Pei, J. *J. Am. Chem. Soc.* **2014**, *136*, 3764–3767. (f) Wang, X.; Zhuang, F.; Wang, X.; Cao, X.; Wang, J.; Pei, J. *Chem. Commun.* **2015**, *51*, 4368–4371. (g) Neue, B.; Araneda, J. F.; Piers, W. E.; Parvez, M. *Angew. Chem., Int. Ed.* **2013**, *52*, 9966–9969. (h) Nakatsuka, S.; Yasuda, N.; Hatakeyama, T. *J. Am. Chem. Soc.* **2018**, *140*, 13562–13565. (i) Hatakeyama, T.; Hashimoto, S.; Seki, S.; Nakamura, M. *J. Am. Chem. Soc.* **2011**, *133*, 18614–18617. (j) Wang, X.; Zhang, F.; Liu, J.; Tang, R.; Fu, Y.; Wu, D.; Xu, Q.; Zhuang, X.; He, G.; Feng, X. *Org. Lett.* **2013**, *15*, 5714–5717. (k) Wang, X.; Zhang, F.; Gao, J.; Fu, Y.; Zhao, W.; Tang, R.; Zhang, W.; Zhuang, X.; Feng, X. *J. Org. Chem.* **2015**, *80*, 10127–10133. (l) Zhang, W.; Zhang, F.; Tang, R.; Fu, Y.; Wang, X.; Zhuang, X.; He, G.; Feng, X. *Org. Lett.* **2016**, *18*, 3618–3621. (m) Kaehler, T.; Bolte, M.; Lerner, H.; Wagner, M. *Angew. Chem., Int. Ed.* **2019**, *58*, 11379–11384.
- (5) (a) Boden, B. N.; Jardine, K. J.; Leung, A. C. W.; MacLachlan, M. *J. Org. Lett.* **2006**, *8*, 1855–1858. (b) Li, J.; Chang, H.; Feng, C.; Wu, Y. *Org. Lett.* **2016**, *18*, 6444–6447. (c) Kaleta, J.; Mazal, C. *Org. Lett.* **2011**, *13*, 1326–1329. (d) Bera, K.; Sarkar, S.; Jalal, S.; Jana, U. *J. Org. Chem.* **2012**, *77*, 8780–8786. (e) Kovács, A.; Vasas, A.; Hohmann, J. *Phytochemistry* **2008**, *69*, 1084–1110.
- (6) (a) Dewar, M. J. S.; Kubba, V. P.; Pettit, R. *J. Chem. Soc.* **1958**, 3073–3076. (b) Dewar, M. J. S.; Kaneko, C.; Bhattacharjee, M. K. *J. Am. Chem. Soc.* **1962**, *84*, 4884–4887.
- (7) (a) Abengózar, A.; García-García, P.; Sucunza, D.; Frutos, L. M.; Castaño, O.; Sampedro, D.; Pérez-Redondo, A.; Vaquero, J. *J. Org. Lett.* **2017**, *19*, 3458–3461. (b) Abengózar, A.; Fernández-González,
- M. A.; Sucunza, D.; Frutos, L. M.; Salgado, A.; García-García, P.; Vaquero, J. *J. Org. Lett.* **2018**, *20*, 4902–4906. (c) Abengózar, A.; Sucunza, D.; García-García, P.; Vaquero, J. *J. Beilstein J. Org. Chem.* **2019**, *15*, 1257–1261. (d) Abengózar, A.; García-García, P.; Sucunza, D.; Sampedro, D.; Pérez-Redondo, A.; Vaquero, J. *J. Org. Lett.* **2019**, *21*, 2550–2554. (e) Abengózar, A.; Sucunza, D.; García-García, P.; Sampedro, D.; Pérez-Redondo, A.; Vaquero, J. *J. Org. Chem.* **2019**, *84*, 7113–7122.
- (8) Bosdet, M. J. D.; Jaska, C. A.; Piers, W. E.; Sorensen, T. S.; Parvez, M. *Org. Lett.* **2007**, *9*, 1395–1398.
- (9) Lu, J.; Ko, S.; Walters, N. R.; Kang, Y.; Sauriol, F.; Wang, S. *Angew. Chem., Int. Ed.* **2013**, *52*, 4544–4548.
- (10) Zhang, C.; Zhang, L.; Sun, C.; Sun, W.; Liu, X. *Org. Lett.* **2019**, *21*, 3476–3480.
- (11) Zhang, J. Y.; Liu, F. D.; Sun, Z.; Li, C. L.; Zhang, Q.; Zhang, C.; Liu, Z. Q.; Liu, X. G. *Chem. Commun.* **2018**, *54*, 8178–8181.
- (12) Schleyer, P. v. R.; Maerker, C.; Dransfeld, A.; Jiao, H.; van Eikema Hommes, N. J. *R. J. Am. Chem. Soc.* **1996**, *118*, 6317–6318.
- (13) (a) Allen, F. H.; Kennard, O.; Watson, D. G.; Brammer, L.; Orpen, A. G.; Taylor, R. *J. Chem. Soc., Perkin Trans. 2* **1987**, S1–S17. (b) Abbey, E. R.; Zakharov, L. N.; Liu, S.-Y. *J. Am. Chem. Soc.* **2008**, *130*, 7250–7252.
- (14) (a) Pan, J.; Kampf, J. W.; Ashe, A. J., III *Org. Lett.* **2007**, *9*, 679–681. (b) Molander, G. A.; Wisniewski, S. R. *J. Org. Chem.* **2014**, *79*, 6663–6678.
- (15) (a) Mottishaw, J. D.; Erck, A. R.; Kramer, J. H.; Sun, H. R.; Koppang, M. *J. Chem. Educ.* **2015**, *92*, 1846–1852. (b) Dunnington, B. D.; Schmidt, J. R. *J. Chem. Theory Comput.* **2012**, *8*, 1902–1911. (c) Reed, A. E.; Curtiss, L. A.; Weinhold, F. *Chem. Rev.* **1988**, *88*, 899–926.
- (16) (a) Corbet, J.; Mignani, G. *Chem. Rev.* **2006**, *106*, 2651–2710. (b) Jana, R.; Pathak, T. P.; Sigman, M. S. *Chem. Rev.* **2011**, *111*, 1417–1492.
- (17) (a) Brown, A. N.; Li, B.; Liu, S.-Y. *J. Am. Chem. Soc.* **2015**, *137*, 8932–8935. (b) Huang, H.; Zhou, Y.; Wang, M.; Zhang, J.; Cao, X.; Wang, S.; Cao, D.; Cui, C. *Angew. Chem., Int. Ed.* **2019**, *58*, 10132–10137. (c) Sun, F.; Lv, L.; Huang, M.; Zhou, Z.; Fang, X. *Org. Lett.* **2014**, *16*, 5024–5027. (d) Zhuang, F. D.; Han, J. M.; Tang, S.; Yang, J. H.; Chen, Q. R.; Wang, J. Y.; Pei, J. *Organometallics* **2017**, *36*, 2479–2482.
- (18) The Stille cross coupling of **1Br-8/2Br-8** with tributyl(4-hexylphenyl)stannane (using $Pd(PPh_3)_4$ as a catalyst and toluene as a solvent) resulted in a low yield as well.
- (19) In the case of the Suzuki cross coupling of **2Br-8** with phenyl boronic acid, the byproduct (**2Ph-8'**, B-OH) was isolated and unambiguously confirmed by X-ray crystal analysis (Tables S21–S23).